MAUSAM, **74**, 1 (January, 2023), 29-42

MAUSAM

DOI : https://doi.org/10.54302/mausam.v74i1.875
Homepage: https://mausamjournal.imd.gov.in/index.php/MAUSAM

UDC No. 551.583:551.524:551.577.36 (540.27)

Estimation of anomalies and temporal temperature and precipitation trends in the Cryospheric Himalayan Highland Region (CHHR), Uttarkashi, Uttarakhand, India

BINDHY WASINI PANDEY, VIRENDER SINGH NEGI*, SUBHASH ANAND, OM JEE RANJAN**, GANESH YADAV*** and SHORYABH SRIVASTAVA

Department of Geography, Delhi School of Economics, University of Delhi, Delhi – 110 007, India

**Department of Geography, Shaheed Bhagat Singh (Evening) College, University of Delhi, Delhi – 110 017, India*

***Department of Geography, Miranda House, University of Delhi, Delhi – 110 007, India*

****Department of Geography, Shaheed Bhagat Singh College, University of Delhi, Delhi – 110 017, India*

(*Received 31 July, 2021, Accepted 28 September, 2022*)

e mails :bwpdsegeo@gmail.com; negivirens@gmail.com; sanandpv@yahoo.co.in; omjeeranjan@gmail.com; ganegeo@gmail.com; shoryabhgeodse@gmail.com

सार – वर्तमान अध्ययन में वर्षा और तापमान के बीच के संबंधों और भिन्नताओं तथा और क्रायोस्फीयर हिमालयी हाइलैंड क्षेत्र (सीएचएचआर)में क्रायोस्फीयर और क्रायोस्फीयर की गतिशीलता पर इसके प्रभाव का पता लगाने का प्रयास किया गया है वर्ष 1981 और 2019 के बीच वर्षा और तापमान डेटा एकत्र किया गया है और मान-केंडल प्रवृत्ति परीक्षण ($\alpha \leq 0.05$; $\alpha \leq 0.10$), और सेन की ढलान का उपयोग करके प्रवृत्ति विश्लेषण किया गया है। वर्षा विसंगति सूचकांक (PAI) की गणना अस्थायी पैटर्न और वर्षण की विविधताओं को समझने के लिए की गई और 39 वर्षों में वर्षा में एक ही प्रवृत्ति पाई गई । मासिक, ऋतुनिष्ठ और वार्षिक तापमान विसंगतियों की भी गणना की गई और यह देखा गया कि शीतलन और उष्णन चक्रों का एक अलग पैटर्न रहा। रैखिक समाश्रयण का उपयोग करके ऋतुनिष्ठ और वार्षिक औसत तापमान तथा वर्षा की गणना की गई और यह पाया गया कि मार्च-अप्रैल-मई (MAM) और जून-जुलाई-अगस्त (JJA) के मौसमों में R^2 सक्रिय रहा है। NDSI और LST की गणना की गई जिसके मानों से पता चलता है कि वर्षों से बर्फ के पिघलने में तेजी आ रही है। यह अध्ययन मध्य-हिमालयी क्षेत्र में जलवायु परिवर्तन के प्रतिकूल प्रभाव को कम करने के लिए उपयुक्त कार्यनीति तैयार करने के लिए उपयोगी है।

ABSTRACT. The present study attempts to explore the variations and linkages between precipitation and temperature and its impact on the Cryosphere Himalayan Highland Region (CHHR) and the dynamics of the cryosphere. The precipitation and Temperature data between the years 1981 and 2019 have been collected and trend analysis is performed using the Mann-Kendell trend test ($\alpha \leq 0.05$; $\alpha \leq 0.10$) and Sen's slope. The Precipitation Anomaly Index (PAI) was computed to understand the temporal patterns and variations of precipitation and there existed a trend in the precipitation over 39 years. Monthly, seasonal and annual temperature anomalies were also calculated and it was observed that there was a distinct pattern of cooling and warming cycles. Seasonal and annual mean temperature and precipitation were calculated using linear regression and it was found that R^2 is robust for MAM and JJA seasons. The NDSI and LST were computed for which values show that the melting of snow has been accelerating over the years. This study is useful for developing appropriate strategies to mitigate the adverse impact of climate change in the mid-Himalayan region.

Key words – Cryosphere, Himalayan highland region, Mann-Kendell, NDSI, LST, Precipitation Anomaly Index (PAI), Anomaly.

1. Introduction

The cryosphere is the abode of snow, ice sheets, glaciers and endless glacial and peri-glacial features. Cryosphere Himalayan Highland Region (CHHR) is considered a Water Tower of the world, from which major rivers originate and drain the fertile land in Asia. Understanding of cryosphere provides the insight to assess mountain ecosystems which is vital for the sustainability of the environment and the livelihood of people at the

local level (Ranjan and Anand, 2017; Ranjan *et al*., 2016, 2020). It is amongst the most fragile environments due to human interferences (Kothawale and Rupa Kumar; 2005). Analysis of long-term data is an appropriate way to learn about variations in climate variables. Climatic indicators like rainfall and temperature have a key role in impacting the entire ecosystem (da Conceição Lima *et al*., 2017; Mishra and Pandey, 2019). Therefore, an analysis of the occurrence of anomalies would be an essential step for understanding climate change outcomes (Ranjan *et al*., 2020). The natural resources in the high altitude regions provide life-supporting, regulating and other vital ecosystem services to locals as well as to downstream people (Pandey *et al*., 2004). These climate anomalies have a deep impact on the natural resources and socio-economic activities of local people in the cryospheric highland. The need and novelty of this study lie in the fact that climate change adaptation is insignificant without understanding the anomalies in the climatic components of the mountain environment. (Duan and Yao, 2003; Chase *et al*., 2003; Pielke, 2002).

The spatial-temporal changes in temperature, precipitation and snow cover alter the livelihood options and lifestyle in cryosphere highland (Chase *et al*., 2003; Duan and Yao, 2003; Pielke *et al*., 2007). The variations in all forms of precipitation and fluctuations in surface temperature have been experienced over the last couple of decades in the Mid-Himalayan Region (Kothawale and Rupa Kumar; 2005). Cryosphere dynamics assessment can provide meaningful insights into adaptive strategies for changing ecological conditions (Khadka *et al*., 2020; Tahir *et al*., 2011). Hence, the monitoring and analysis of anomalies in climatic indicators in cryosphere highland and the correlation between precipitation and temperature are the main objectives of the present study.

2. The study area

The study area is the Uttarkashi district in Uttarakhand, India. It lies between 30° 28' N to 31° 28' N and 77° 49' E to 79° 25' E (Fig. 1). It covers an area of 8016 sq km. The altitude varies between 1200 m to 7000m. Uttarkashi has a rugged topography with huge anticlines and synclines of the middle Himalayas. It is surrounded by Tibet (China) and Himachal Pradesh from the North, Tehri district from the South, Chamoli and Rudraprayag district from the Eastern side and Dehradun district in the west.

It is the largest district of Uttarakhand as per the total area. The general elevation of the region varies from 850 m to 7000 m. The mean temperature varies from near 0 °C during winters to 35 °C during summers. This is

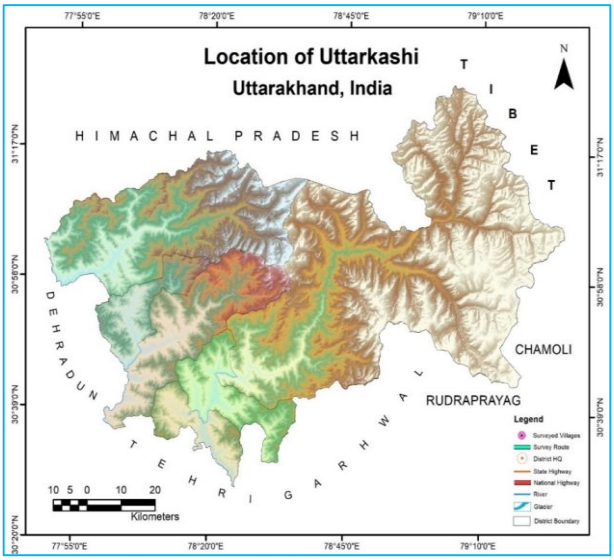

Fig. 1. Location map of study area
Source : Prepared by authors using Cartosat-1, Bhuvan, 2021

followed by monsoons and post Monsoon Seasons (October to December) (IMD, 2021). The Northern part of the district is snow-covered throughout the year with a Sub-arctic type climate.

Since the location of the study area is in the middle Himalayas, population distribution is largely sparse and isolated in clusters. According to the 2011 Census, the population of Uttarkashi district is 330,086 which are 3.27 Per cent of the total population of the state. The sex ratio of the district is 958 which are below the state average of 963. Population Density is only 3/km^2 whereas the literacy rate stands at 77.20 per cent. Male and female literacy is 86.31 per cent 63.56 Per cent, respectively (Census of India, 2011).

3. Dataset and methodology

Data for the study have been collected from the National Aeronautics and Space Administration's (NASA) as the open data source. The data includes long-term (39 years), from 1981 to 2019, climatology data on precipitation and temperature. This data has been retrieved from the NASA Power Project from the grid having a spatial resolution of 0.5° latitude by 0.5° longitude. The trend analysis on the climatological data is useful to understand the Spatio-temporal patterns and variations of temperature and rainfall (Longobardi and Villani, 2010).

The Spatio-temporal patterns and trends were analysed by the Mann-Kendall test. The Mann-Kendall test was developed by Mann (1945) as a non-parametric test (Lehmann, 1975) to analyse the variations of Spatio-

temporal trends and patterns. In addition, the anomaly was calculated using a Z score to see the deviation of values from the long term average.

3.1. *The Man-Kendell formula has been applied for the calculation is :*

$$S = \sum_{i=1}^{n-1} \sum_{j=i+1}^{n} \operatorname{sgn}\left(x_j - x_i\right) \quad (1)$$

where, n = data points; x_i and x_j = data values; i and j = time series

$$\operatorname{sgn}\left(x_j - x_i\right) = \begin{cases} +1 \text{ if } x_j - x_i > 0 \\ 0 \quad \text{if } x_j - x_i = 0_n \\ -1 \text{ if } x_j - x_i < 0 \end{cases} \quad (2)$$

3.2. *Calculation of Anomaly*

$$\zeta = \frac{x_i - \mu}{\sigma} \quad (3)$$

In the above-mentioned equation,

ζ = Standardised Anomaly; x_i = Observations; μ = mean of observations; σ = Standard deviation.

3.3. *Calculation of Sen's slope*

To calculate the slope of trend in the data having n pairs, a non-parametric procedure developed by Sen (1968) was utilized. A linear model was utilized in Sen's equation to calculate the trend of the slope using:

$$Q_i = \frac{X_j - X_k}{j - k} \text{ for } i = 1,..., n \quad (4)$$

where,

X_j-X_k = data values at times j and k (j>k)

For one Datum = $N = n(n - 1)/2$ or,

Multiple Data = $N<n(n - 1)/2$

The n values of Q_i are ranked from smallest to largest and the median of slope or Sen's slope estimator is calculated as :

$$Q_{med} = \begin{cases} Q_{\left[\frac{n+1}{2}\right]}, & \text{if } n \text{ is odd} \\ \dfrac{Q_{\left[\frac{n}{2}\right]} + Q_{\left[\frac{n+2}{2}\right]},}{2} & \text{if } n \text{ is even} \end{cases} \quad (5)$$

TABLE 1

Precipitation Anomaly Index for Uttarkashi district between 1981 to 2019

	PAI Range	Classification
Precipitation Anomaly Index (PAI)	Above 4	Extreme Precipitation
	2 to 4	Heavy Precipitation
	0 to 2	Average Precipitation
	-2 to 0	Less Precipitation
	Below -4	Extremely Less Precipitation

Source : Computed by the Authors, Adapted from Freitas (2005)

To calculate the confidence interval of the time slope one can go for the formula:

Eq. 2

$$C_\alpha = Z_{1-\alpha/2}\sqrt{Var(S)} \quad (6)$$

3.4. *Precipitation Anomaly Index (PAI) calculation*

From the data obtained for the precipitation, the Precipitation Anomaly Index (PAI) was used to analyse the variation in the intensity of the precipitation over some time. The PAI used for the calculation of the intensity of precipitation between 1981 to 2019 is based upon the Rainfall Anomaly Index (RAI) developed by Van Rooy (1965) (Machiwal *et al*., 2016; Costa & Rodrigues, 2017) and it was later adopted by Freitas (2005). The following formula was used for the calculation of the PAI:

$$\text{PAI} - 3\left[\left[\frac{N - \bar{N}}{\bar{M} - \bar{N}}\right]\right] \text{ for positive anomalies} \quad (7)$$

Eq. 4

$$\text{PAI} - 3\left\|\frac{N - \bar{N}}{\bar{X} - \bar{N}}\right\| \text{ for negative anomalies} \quad (8)$$

where,

N = yearly rainfall
$\bar{N}$ = yearly average rainfall of the historical series (mm)
$\bar{M}$ = average of the ten highest monthly/yearly precipitations of the historical series (mm)
$\bar{X}$ = average of the ten lowest monthly/yearly precipitations of the historical series (mm)

Based on PAI scores**,** different categories were formed. PAI closer to 0 is indicative of average rainfall, whereas the greater difference is reflective of extreme climatic events like drought and flood (Table 1).

3.5. *Relationship between temperature and precipitation*

To analyse the relationship between temperature and precipitation, simple linear regression was applied for understanding the mean annual and mean seasonal relationships of temperature and precipitation. Regression was calculated using the following formula;

$$y = \alpha + \beta x \tag{9}$$

where, y is the dependent variable, x is the independent variable, α is the y-intercept and β is the slope.

In this analysis, the mean temperature (The X variable) is the independent variable whereas the precipitation (The Y variable) is dependent. A Scatter plot has also been used to see the interrelation of observations.

Z score enabled to compare two scores having different means and standard deviations. The formula utilized to calculate Z scores for anomalies where x is the raw score, μ is the mean and σ is the standard deviation.

$$Z = \frac{x - \mu}{\sigma} \tag{10}$$

The value of the z-score revealed the number of standard deviations from which the variables are away from the mean. If a *z-score* is equal to 0, its means value is on the mean point. A positive value of *z-score* indicates that the raw score is comparatively higher than the mean value and a negative Z score indicates the raw score to be lower than the mean average. Anomalies were plotted to see the linear combination of anomalies for temperature and precipitation.

3.6. *For the calculation of Land Surface Temperature (LST)*

Following formula has been used accordingly, (Zhengming and Dozier, 1996; Sekertekin, 2019).

For Landsat 5 TM

Step 1 *Conversion DN to Radiance*

$$L\lambda = \left[\left(LMAX\lambda - LMIN\lambda\right)/\left(QCALMAX - QCALMIN\right) * \left(QCAL - QCALMIN\right) + LMIN\lambda\right] \tag{11}$$

where,

$L\lambda$ = Spectral radiance at the sensor's aperture in [Watts/(m² * sr * µm)] Quant. and Calibrated Std. is in Digital nos.

$LMIN\lambda$ = Spectral radiance scaled to QCALMIN in [Watts/(m² * sr * µm)]

$LMAX\lambda$ = Spectral radiance scaled to QCALMAX in [Watts/(m² * sr * µm)]

$QCALMIN$ = Minimum quantized calibrated pixel value (correspondingly to L Minimum λ) in Digital No. = 1

$QCAL$ = Maximum is also in Digital values = 255

Step 2 *Conversion of Spectral Radiance to Temperature (In kelvin)*

$$T = \frac{K2}{\ln\left(\frac{K_1}{L_\lambda} + 1\right)} \tag{12}$$

where,

T = Effective at-satellite temperature in Kelvin

K2 = Calibration constant 2

K_1 = Calibration constant 1

L_λ = Spectral radiance in watts/(meter squared * ster * µm)

After then retrieved temperature unit has been converted from kelvin to Degree Celsius

For Landsat-8 OLI/TIRS **(**Sekertekin, 2019; García-Santos *et al*., 2018)

Step 1 *Conversion DN to Radiance*

$$L\lambda = MLQcal + AL \tag{13}$$

$L\lambda$ = Spectral radiance [W/ (m^2 * sr * µm)]

ML = Radiance multiplicative scaling factor for the band

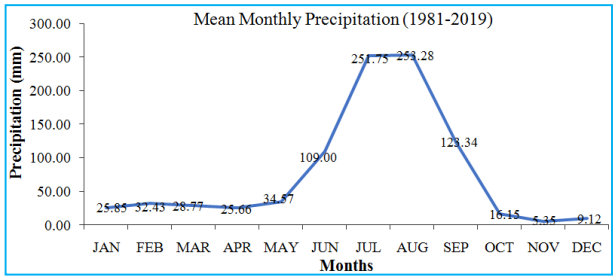

Fig. 2. Mean Monthly Precipitation in Uttarkashi District, 1981-2019. *Source* : Computed by the Authors, 2021

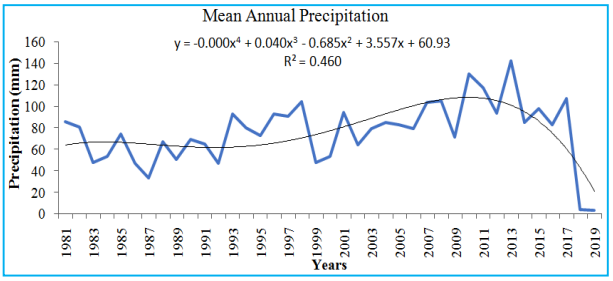

Fig. 3. Mean Annual Precipitation in Uttarkashi District, 1981-2019. *Source* : Prepared by the Authors, 2021

AL is showing Radiance additive scaling factor for the band

Q Cal. = Level 1 pixel value in Digital Nos.

Step 2 *Conversion of Spectral Radiance to Temperature (In kelvin)*

$$T = \frac{K_2}{\ln\left(\frac{K_1}{L_\lambda}+1\right)} \qquad (14)$$

where

T = Effective at-Satellite temperature (in K)

K_2 = Calibration constant 2

K_1 = Calibration constant 1

L_λ = Spectral Radiance (in W) after the temperature unit has been converted from K to °C

Step 3 *Convert Temperature (In kelvin) to Degree Celsius*

°C = K – 273.15

3.7. For the calculation of the *Normalized Difference Snow Index (NDSI)* following formula has been adopted: (Valovcin, 1978; Durán-Alarcón *et al*., 2015; Hall & Riggs, 2011; Hauser & Schmitt, 2021).

$$\text{NDSI} = \frac{\text{Green} - \text{SWIR}}{\text{Green} + \text{SWIR}} \qquad (15)$$

To calculate the NDSI from Landsat 5 TM band 2 (Green) and band 5 (SWIR) were used for 2000, 2010. In Landsat 8 OLI/TIRS Green and SWIR Bands used for 2020 (Hauser & Schmitt, 2021).

4. Results and discussion

4.1. *Mean monthly precipitation*

Mean monthly precipitation for the taken period 1981 to 2019, has been plotted to see the pattern of precipitation. Over the years, it has been observed that Uttarkashi receives the lowest amount of precipitation in November (5.35 mm), followed by December (9.12 mm) and October (16.15 mm) (Fig. 2). Most of the precipitation in January and February comes in the form of snowfall and is supplied by fresh snow or glaciers. The maximum amount of precipitation occurs during the monsoon, *i.e*., in August (253.28 mm) and July (257.75 mm) (Fig. 2). This huge amount of rainfall during monsoon triggers flashfloods, landslides and rockfall in this high altitude and removes the thin soil cover (Pandey, 2002).

4.2. *Mean annual precipitation*

The mean distribution of precipitation over 39 years (1981-2019) in the Uttarkashi District has been studied. The Average Annual Precipitation of Uttarkashi District over 39 (1981-2019) years is estimated at 913.37 mm. The maximum amount of rainfall happened in 2014. There is a fluctuation in precipitation almost every year since 1981. But the long term polynomial trend line over the same period shows that there is a gradual increase in precipitation from 1981 till 2014, from then the precipitation is falling every year (Fig. 3).

4.3. *Mann-Kendall Test for the mean annual precipitation*

The data for 39 years was collected and analysed for the maximum and minimum precipitation. This shows that Uttarkashi district received minimum precipitation of

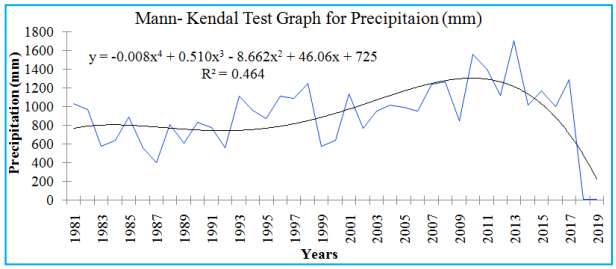

Fig. 4. Mann-Kendall Trend Test Graph for Prec. (mm) between the years 1981 to 2019.
Source : Prepared by the authors, 2021

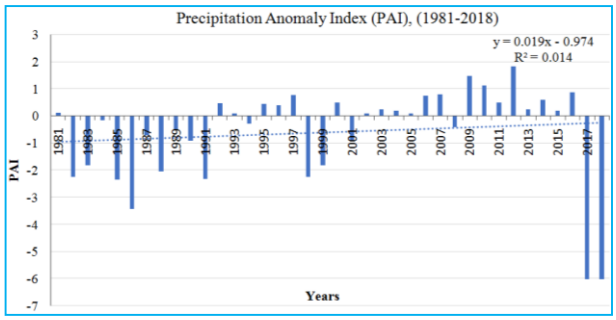

Fig. 5. Annual Precipitation Anomaly Index (PAI) for the Uttarkashi District, 1981-2018.
Source : Computed by the authors, formula adapted from Van Rooy (1965) and Freitas (2005)

TABLE 2

Mann-Kendall trend test / two-tailed test (ANN)

Kendall's tau	0.293
S	217.000
Var(S)	6833.667
p-value (Two-tailed)	0.009
alpha	0.05

Source : Computed by the Authors, 2021

3.060 mm and maximum precipitation of 1705.160 mm over the observance period.

When calculated on the Mann-Kendall trend test to analyse the trend. It was found that the *p*-value of the test was lower than the significance level alpha = 0.05. One should reject the null hypothesis H_0 and accept the alternative hypothesis Ha (Table 2). Where, it is very important to note that H_0 signifies the null hypothesis that says that there existed no trend in the precipitation between 1981 to 2019 that prefers rejecting H_a that is the alternative hypothesis that denotes that there existed a trend in the precipitation between 1981 and 2019.

The *p*-value is computed using the exact method of the Mann-Kendall test and it was found the risk of rejecting the null hypothesis H_0 while it is true that it is lower than 0.90 per cent. Therefore, one can see that there is a trend in the precipitation between 1981 to 2019 (Fig. 4).

4.4. *Precipitation Anomaly Index (PAI)*

The following graph in Fig. 4 represents an upward trend in precipitation in the years 1981, but in 2017 and 2018 the precipitation decreased sharply in the district. To see the changes in the variation the precipitation anomaly was also calculated.

Fig. 5 indicates that there are absolutely no cases of extreme rainfall and heavy precipitation in the last 39 years. Out of the 39 years of precipitation, 17 years (1983, 1984, 1987, 1988, 1989, 1990, 1994, 1999, 2001, 2008, 1982, 1985, 1986, 1991, 1998, 2017 and 2018) are the years when the precipitation was less than the average. In 2017 and 2018 the precipitation received in the district was average. A similar situation was recorded in 1986 when the precipitation was far below the average (Table 3). It is to be noted that authors have left 2019 for PAI analysis due to insufficient climatic data recorded for the period.

4.5. *Mean temperature*

The month-wise mean temperature range distribution in the Uttarkashi district reveals that the district records the highest temperature in June that goes up to 24 °C. The minimum average temperature in the district goes near -1.59 °C in January.

Similarly, the annual average temperature between 1981-2019 reveals that the annual average temperature of 39 years remained firm within the range of 10.79 °C to near 13.32 °C. The mean annual temperature trend using the polynomial trend line shows that mean temperature increased sharply after 1981 and had its peak in 1988 and then we observe a steady decline of the temperature till 1997. From 1997 till 2017, the temperature is stable but post 2017, there is a slight decline.

4.6. *Temperature anomalies*

Mean temperature anomalies reflect the deviation of mean temperature for a particular month the observation from 39 years' average temperature has been calculated. An anomaly near zero implies that values are near to the mean and *vice versa*. Monthly temperature anomalies for each month and all the 12 months have been depicted in the graph and it shows that for January, the year 1988,

TABLE 3

Precipitation Anomaly Index for Uttarkashi district between 1981 to 2018

	PAI Range	Classification	Results
Precipitation Anomaly Index (PAI)	Above 4	Extreme Precipitation	-
	2 to 4	Heavy Precipitation	-
	0 to 2	Average Precipitation	1981, 1992, 1993, 1995, 1996, 1997, 2000, 2002, 2003,2004, 2005, 2006, 2007, 2009, 2010, 2011, 2012, 2013, 2014, 2015, 2016
	-2 to 0	Less Precipitation	1983, 1984, 1987, 1988, 1989, 1990, 1994, 1999, 2001, 2008
	-2 to -4	Very less Precipitation	1982, 1985, 1986, 1991, 1998
	Below -4	Extremely Less Precipitation	2017, 2018

Results are arranged based on the decreasing amount of precipitation by year

Source : Computed by the Authors, Adapted from Freitas (2005), 2021

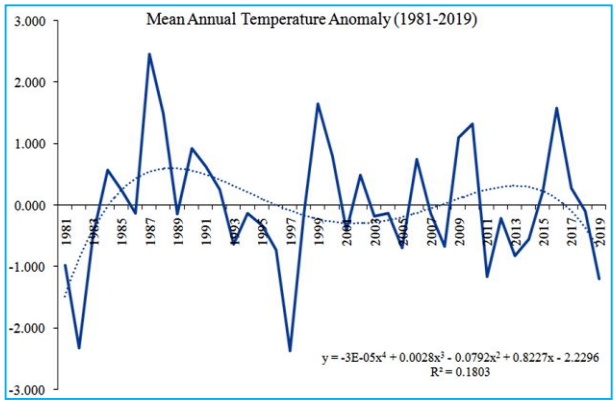

Fig. 6. Mean Annual Temperature Anomaly in Uttarkashi District, 1981-2019. *Source* : Computed by the Authors,2021

1990, 1992, 2000, 2003, 2006, 2007, 2009 and 2016 were warmer whereas 1989, 1995, 2011, 2012 and 2019 were significantly colder. The polynomial trendline since 1981 is an increasing trend till 1995 and there is a stable trend thereafter until 2016. After 2016, there is a decrease till 2019.

The month of February 2006 was significantly warmer than other years whereas in the years 2000, 2014 and 2019 it was colder than the average. The trend analysis shows that since 2005, there is an increasing trend in mean temperature till 2016 and afterwards it shows a declining trend. For March, the year 1984, 1985, 2004 and 2010 were significantly warmer. The polynomial trend line shows that since 1998, the average temperature is showing an increasing trend till 2016 from which it is declining. For April 1982 was significantly colder whereas 2010 was the warmest till now. Trendline analysis reflects that April is warmer from 1999 to 2016 and afterwards it is getting colder. The month of May was significantly warmer in 1984, 1988, 2000, 2010 and 1988 while the same is much colder in 1982 and 1997. The trendline analysis shows that since 1985, the temperature is above from mean till 2000 when it became stable and started rising again until 2016 after which the month is getting relatively colder. The hottest June was recorded in the year 1990 whereas the coldest was in 2011. The month was warmer from 1982 till 1999 and later it is relatively colder (Fig. 7). The month of July shows the same trend as of June, the month is warmer from 1981 till 1998 afterwards it is colder. The warmest August was recorded in 1987 whereas the coldest one was in 2008. This month is warmer till 1999 and later it is colder but the temperature is nearing to mean after 2016. The month of September is warmest in 1987 and 1999 and the polynomial trend line shows that year from 1984 till 1995 is warmer than it becomes colder till 2010 and again warmer during post-2010.

The trend for October over the years shows that since 1983, it was warmer till 1991 afterwards until 2006 the month was colder and since then again it is getting warmer nevertheless the difference is getting smaller for the mean temperature. The month of November was significantly warmer in 2015 whereas it was much colder in 1981. The polynomial trendline analysis shows that it is getting warmer after 2006. 2016 was the warmest month and the coldest in 1981. Since 2000, this month is getting warmer till 2012, after which it shows a decreasing trend (Fig. 7).

The overall mean annual temperature anomaly shows that 1987 was the hottest recorded year whereas 1997 is the coldest recorded year till now. Other significantly warmer years are 1999, 2002, 2006, 2009, 2010, 2015,

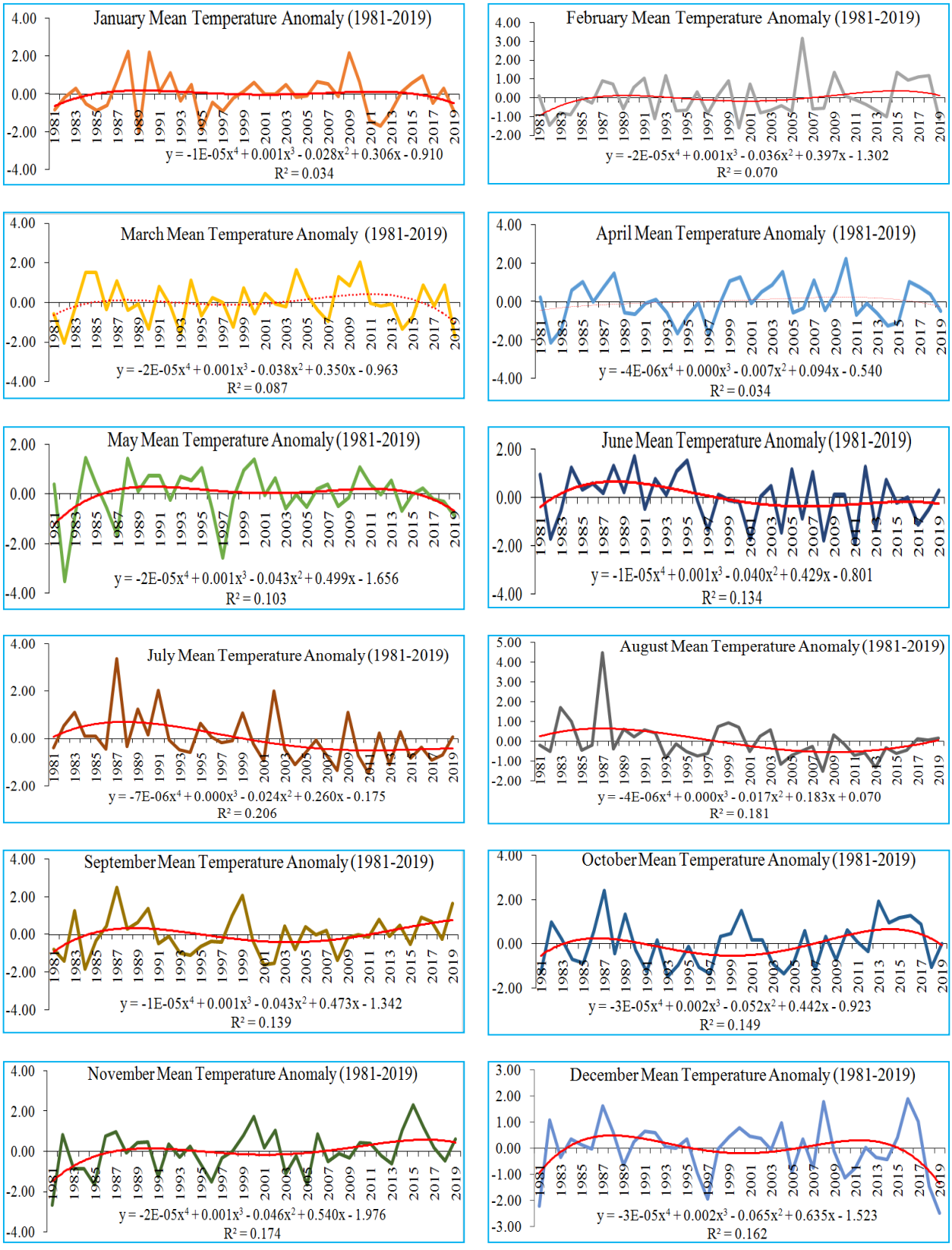

Fig. 7. Mean Monthly Temperature Anomaly in Uttarkashi District, 1981-2019. *Source* : Computed by the Authors, 2021

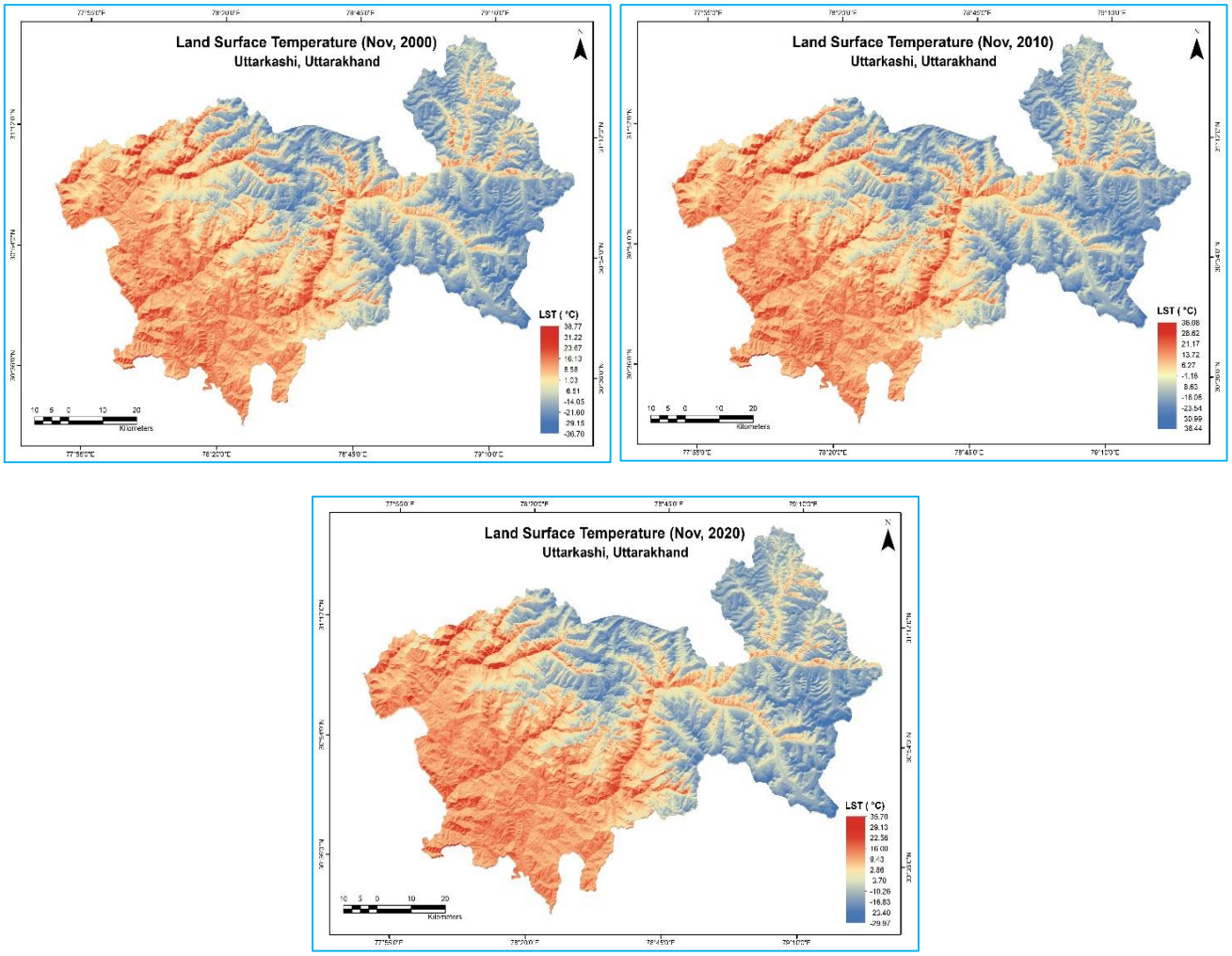

Fig. 8. Land Surface Temperature of Uttarkashi District, 2000, 2010 and 2020.
Source : Landsat 5TM and Landsat 8OLI/TIRS, Retrieved from USGS Portal, Computed on ArcGIS 10.3 by the Research Team, 2021

2016 and 2017. Other significantly colder years are 1993, 1982, 2001, 2003, 2004, 2005, 2008, 2011, 2012, 2013, 2014, 2018 and 2019. The overall trend analysis using polynomial regression shows that from 1981 to 1983 there was a negative anomaly trend, which became positive till 1996. From 1996, it again became negative till 2007 and positive thereafter till 2017. The trend after 2017 shows a negative anomaly which implies that it is getting cooler lately (Fig. 6).

4.7. *LST change over time*

Calculation of the land surface temperature of the study area can help in identifying the influence of climatic variables on the cryospheric highland of the Uttarkashi district. The Land Surface Temperature (LST) of the district was calculated for the years 2000, 2010 and 2020 (Fig. 8). Retrieved data showed the minimum temperature in the district in the year 2000 was about -36.70 °C and that further decreased to -38.44 °C by the year 2010. It was further observed that the minimum temperature of the district increased to -29.97 °C by the year 2020. The maximum temperature in the district in the year 2000 was 38.77 °C that decreased to 36.08 °C by the year 2010 and further decreased to 35.70 °C by the year 2020 (Fig. 8). Therefore, LST analysis shows that there are fluctuations in LST over the years as evident from climatic data analysis as well.

4.8. *Relationship between temperature and precipitation in the study area*

The simple linear regression model was used to see the relationship between temperature and precipitation for seasonal and annual trends. The seasonal trend was analysed for all IMD designated seasons of December-

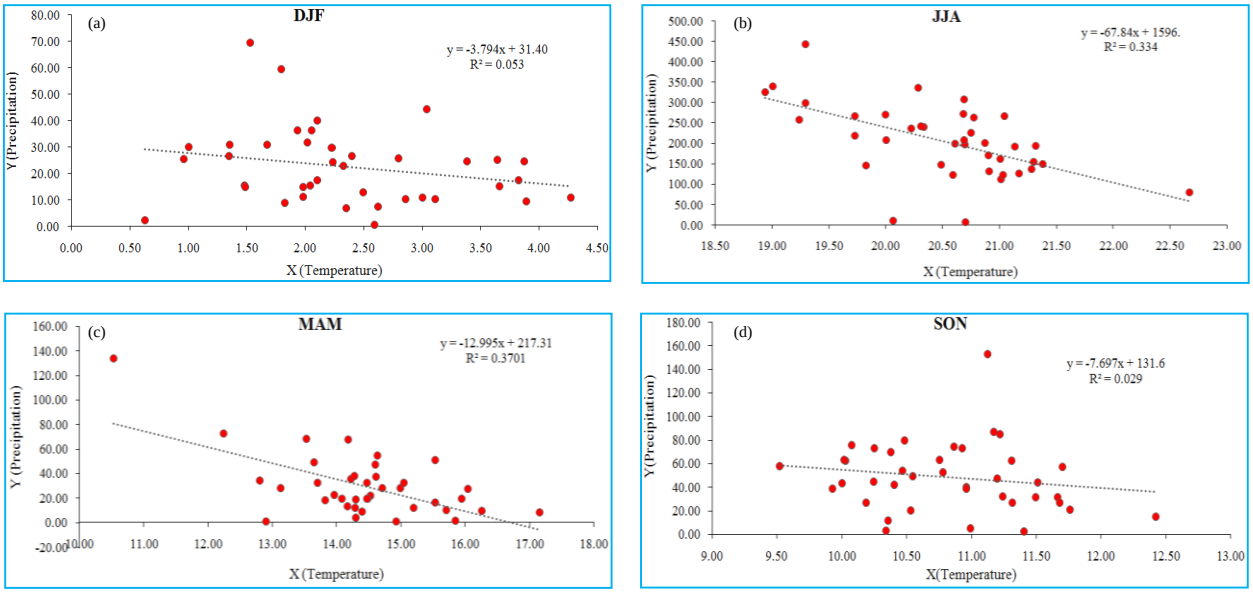

Figs. 9(a-d). Relationship between Seasonal Temperature and Precipitation in Uttarkashi District, 1981-2019. *Source* : Computed by the Authors, 2021

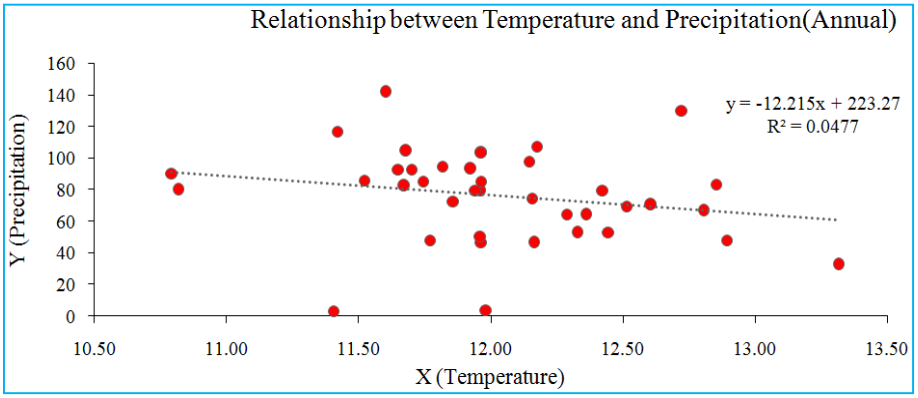

Fig. 10. Relationship between Annual Temperature and Precipitation in Uttarkashi District, 1981-2019. *Source* : Computed by the Authors, 2021

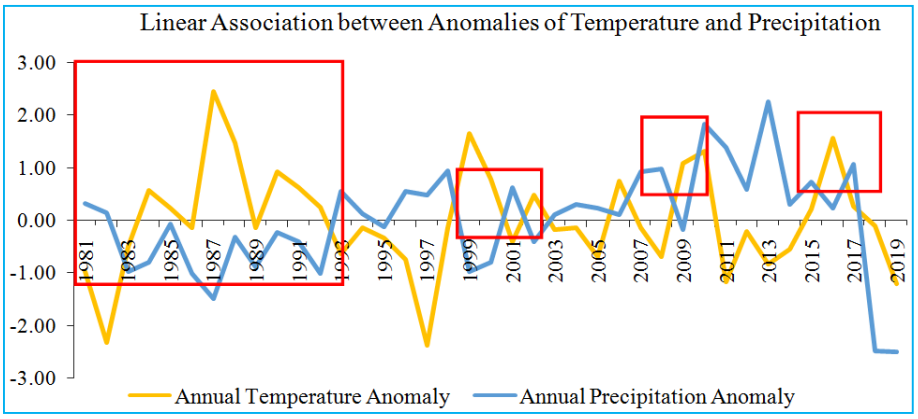

Fig. 11. Linear Relationship between Annual Temperature and Precipitation Anomalies in Uttarkashi District, 1981-2019. *Source* : Computed by the Authors, 2021

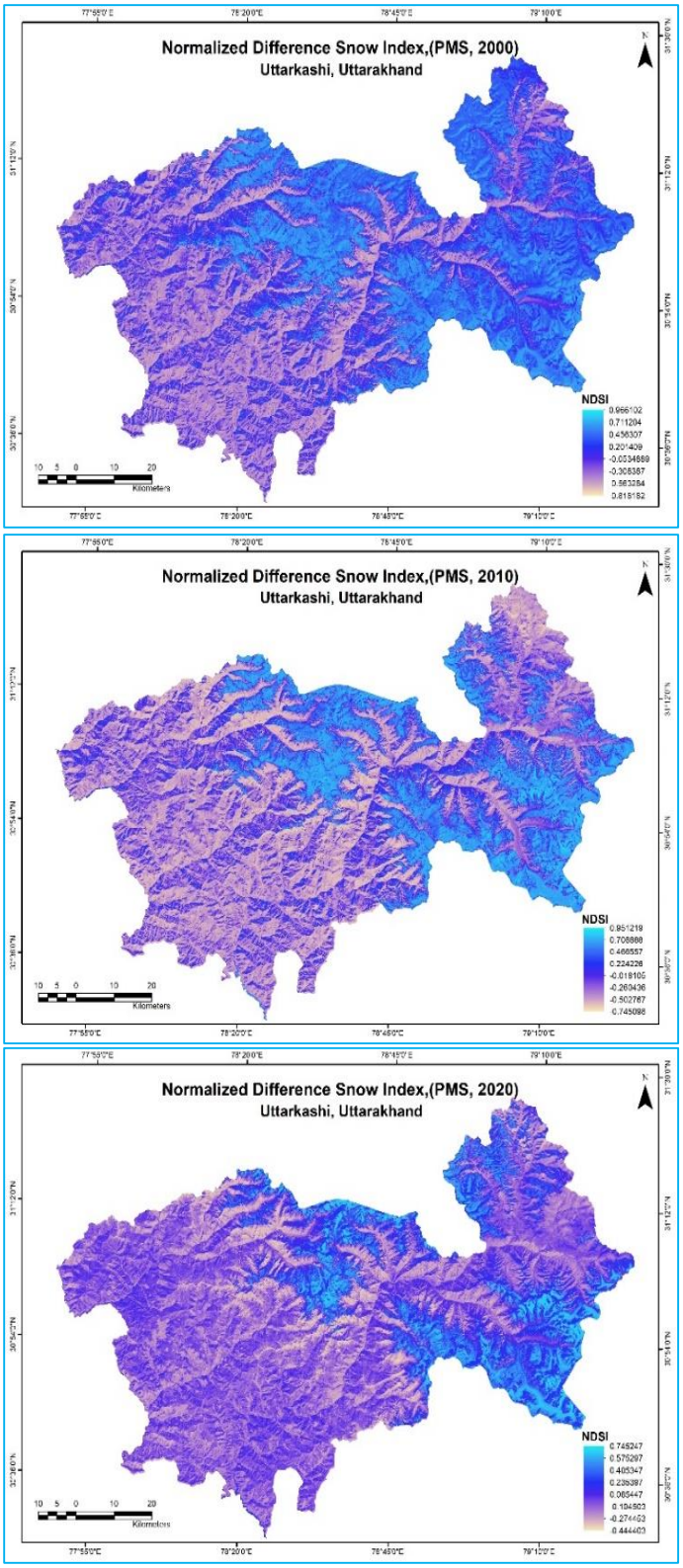

Fig. 12. Normalized Difference Snow Index (NDSI) of Uttarkashi District, 2000, 2010 and 2020. *Source* : Landsat 5TM and Landsat 8 OLI/TIRS, retrieved from USGS Portal, Computed on ArcGIS 10.3 by the Research Team, 2021

January-February (DJF), March-April-May (MAM), June-July-August (JJA) and September-October-November (SON). The relationship of mean temperature with mean precipitation in all the seasons show a negative association, R^2 model is more robust in MAM and JJA as the rainfall is possible only during the summer and rainy seasons in this part of the Himalayas. The value of R^2 is very less during winters (DJF) and autumn (SON). This is particularly due to the amount of precipitation falling in the form of snow. Across the world, it has been observed that temperature is more associated with rainfall trends than snowfall trends. There are other local factors responsible for the weak models including elevation, slope, vegetation, orientation, etc. [Figs. 9(a-d)].

The relationship between annual mean temperature and annual mean precipitation is also negative. The model R^2 is even weaker explaining just 4 percent of the total variation. The major reason for a weak model is that multiple factors are working that determine the amount of precipitation over a year, particularly distant sea surface temperatures, elevation, slope, vegetation, etc. (Fig. 10).

Linear association of mean annual anomalies of temperature and precipitation shows a mixed pattern. And from 1983 till 1995 there is a similarity in the anomalies (Fig. 11).

The similarities were visible again in 2002, 2009-2011 and in 2016-17. In other years the similarities of anomalies were not observed. This might be due to other confounders that impact the pattern of precipitation and temperature over the years (Fig. 11).

4.9. *Impact of Climatic Anomalies on Cryosphere Dynamics*

Normalized Difference Snow Index (NDSI) : Snow plays an important role in deciding the frequency and intensity of hydrological phenomena and ecological risks and hazards (Ranjan *et al*., 2020; Hauser & Schmitt, 2021). In the Uttarkashi district of Uttarakhand, snow is mostly found in the higher elevations and most often this is the reason behind natural hazards like glaciated lake outbursts and floods. The NDSI is an index developed to identify the presence of snow in pixels and is very effective in detecting the snow cover.

The NDSI algorithm explains that values between 0.0 to 1.0 (Fig. 12). The NDSI value for the years 2000, 2010 and 2020 was calculated as 0.97, 0.95 and 0.75, which shows that snow cover is declining slowly in the district of Uttarkashi. The most proximate reason for shrinking snow cover is temperature fluctuations and high variability in precipitation over the years.

5. Conclusions

In the present study, the trend of precipitation anomalies and temperature anomalies has been estimated with the help of daily measured data of 39 years to understand the state of climate change over the long term. Along with this, the data received from satellites were also analysed to verify whether the changing amplitude has any effect on physiography. It was observed that out of the 39 years of precipitation, 17 years witnessed a declining trend than the average precipitation. There were only 2 years when the average precipitation was extremely low. The analysis of temperature anomalies shows that since 1981 there is an increasing trend in temperature till 1995 and thereafter till 2016 temperature pattern is stable. After 2016, the mean annual temperature anomaly is falling till 2019, these trends reflect that there are significant fluctuations over the observed years, strong enough to impact the Cryosphere dynamics. Positive anomalies are reflective of high mean annual temperature over mean long term annual period (1981-2019). This was again validated by NDSI analysis over the years using satellite images that area under the snow coverage has shrunk. Understanding the threshold of these fluctuations is a complex process and there is no universal numerical cut-off point of cryosphere shrinking as other factors such as soil type, rock type, vegetation cover and soil moisture varies from place to place (Tang *et al*., 2014).

Another significant observation was that February in the year 2006 was comparatively warmer than the other years and April month is getting warmer since 1999 and continues to remain so till 2016. It is observed that between temperature and precipitation, a robust negative correlation was identified for the seasons MAM and JJA, computed over the long term average of 30 years. These are typically summer and rainy seasons respectively. In this higher altitude, precipitation mostly occurs in the form of snow. With the increasing temperature, there has been a declining precipitation and hence snow and moisture content. This is also validated by analysing the satellite data and calculating the snowfall index (NDSI) as there is a declining trend of snow cover over the past thirty years.

Therefore, this study on the trends of the precipitation, temperature, land surface temperature and snow cover focuses on their role in understanding the weather patterns and associated changes in the Cryospheric Himalayan Highland Region (CHHR), respectively. The influence of temperature and precipitation anomalies over the years has been reflected in the relatively odd seasonal characteristics and weather patterns. Land Surface temperature and snow cover are subjective to this changing temperature and precipitation

trends and hence changes in the Cryospheric Himalayan Highland Region (CHHR).

Funding

This research paper is an outcome of a Research Project supported and funded by the Institute of Eminence (IoE) the University of Delhi under the FRP Scheme.

We have no conflicts of interest to disclose.

Acknowledgements

The authors are grateful to the Institute of Eminence (IoE) the University of Delhi for supporting this research and providing financial grants under the FRP Scheme. We thank various Government Departments, Institutions and USGS for providing secondary data for the present work.

Disclaimer : The contents and views expressed in this study are the views of the authors and do not necessarily reflect the views of the organizations they belong to.

References

Census of India, 2011, "District Census Handbook of Uttarkashi, Uttarakhand", *Census of India*. Government of India, New Delhi.

Chase, T. N., Knaff, J. A., Pielke, R. A. and Kalnay, E., 2003, "Changes in Global Monsoon Circulation since 1950", *Natural Hazards*, **29**, 229-254.

Costa, J. A. and Rodrigues, G. P., 2017, "Space-Time Distribution of Rainfall Anomaly Index (Rai) For The Salgado Basin", Ceará State - Brazil. *Ciência e Natura*, **39**, 3, 627. https://doi.org/10.5902/2179460x26080.

da Conceição Lima, C., Sousa, J. and Henrique Viana De Freitas, F., 2017, "Um Sistema De Suporte A Decisão Para Planejamento De Redes De Sensores Sem Fio Aquáticas", *Link science place*, **3**, 4, 79-89. https://doi.org/10.17115/2358-8411/v3n4a6.

Duan, K. and Yao, T., 2003, "Monsoon Variability in the Himalayas under the condition of Global Warming", *Journal of the Meteorological Society of Japan*, **81**, 2, 251-257.

Durán-Alarcón, Claudio, Gevaert, C, M., Mattar, C., Jiménez-Muñoz, Juan, C., Pasapera-Gonzales, José J., Sobrino, José A., Silvia-Vidal, Yamina, Fashé-Raymundo, Octavio, Chavez-Espiritu, Tulio W. and Santillan-Portilla, Nelson, 2015, "Recent trends on glacier area retreat over the group of Nevados Caullaraju-Pastoruri (Cordillera Blanca, Peru) using Landsat imagery", *Journal of South American Earth Sciences*, **59**, 19-26. https://doi.org/10.1016/j.jsames.2015.01.006.

Garcia-Santos, V., Cuxart, J., Villagrasa, D. M., Jiménez, M. A. andSimó, G., 2018, "Comparison of Three Methods for Estimating Land Surface Temperature from Landsat 8-TIRS Sensor Data", *Remote Sensing*, **10**, 9, 1450. https://doi.org/10.3390/ rs10091450.

Government of Uttarakhand, Official Website of State Horticulture Mission, Govt. of Uttarakhand. *https://shm.uk.gov.in/pages/display/6-state-profile.* Retrieved on 20.05.2021.

Hall, D. K. and Riggs, G. A., 2011, "Normalized-Difference Snow Index (NDSI)", *Encyclopedia of Earth Sciences Series*, 779-780. https://doi.org/10.1007/978-90-481-2642-2_376.

Hauser, S. and Schmitt, A., 2021, "Glacier retreat in Iceland mapped from SPACE: Time series analysis of geodata from 1941 to 2018", *PFG - Journal of Photogrammetry, Remote Sensing and Geoinformation Science*. https://doi.org/10.1007/s41064-021-00139-y.

Khadka, M., Kayastha, R. B. and Kayastha, R., 2020, "Future projection of cryosphere and hydrologic regimes in Koshi River basin, Central Himalaya, using coupled glacier dynamics and glacio-hydrological models", *Journal of Glaciology*, **66**, 259, 831-845.

Kothawale, D. R. and Rupa Kumar, K., 2005, "On the recent changes in surface temperature trends over India", *Geophysical Research Letters*, **32**. L18714, DOI: 10.1029/2005GL023528.

Lehmann, E. L., 1975, "*Non-parametric, Statistical Methods Based on Ranks*", Holden-Day, San Francisco, California, USA.

Longobardi, A. and Villani, P., 2010, "Trend analysis of annual and seasonal rainfall time series in the Mediterranean area", *International Journal of Climatology*, **30**, 10, 1538-1546. doi : 10.1002/joc.2001.

Machiwal, D., Kumar, S., Dayal, D. and Mangalassery, S., 2016, "Identifying abrupt changes and detecting gradual trends of annual rainfall in an Indian arid region under heightened rainfall rise regime", *International Journal of Climatology*, **37**, 5, 2719-2733. https://doi.org/10.1002/joc.4875.

Mann, H. B., 1945, "Nonparametric tests against the trend", *Econometrica*, **13**, 3, 245-259. doi : 2307/1907187.

Mishra, H. and Pandey, B. W., 2019, "Navigating the Impacts of Social and Environmental Changes to Traditional Lifestyle: A Case Study of Gaddi Transhumance of Chamba District in Himachal Pradesh", *The Oriental Anthropologist*, **19**, 2, 326-337.

Official Web Site of India Meteorological Department (IMD), Pune. (n.d.). Https://www.Imdpune.Gov.in/Weather/Reports/ Glossary. Pdf. Retrieved July 25, 2021, from https://www.imdpune.gov.in/Weather/

Pandey, B. W., 2002, "Geo-environmental Hazards in Himalaya Assessment and Mapping (the Upper Beas Basin), Mittal Publication, New Delhi. 2002. p403.

Pandey, B. W., Bandooni, S. K. and Negi, V. S., 2004, "Community Participation in Water Resources Conservation and Management in Raath Region of Garhwal Himalaya", In G. S. Chauhan and R. N. Dubey (eds.) *Water Resources Management*. Nataraj Publications, New Delhi. 2004. 203-224. ISBN : 81-7312-024-2.

Pielke R. A. Sr., 2002, "The influence of land-use changes and Landscape Dynamics on the Climate System-Relevance to climate change policy beyond the Radiative effect of Greenhouse gases", *Philosophical Transactions of the Royal Society of London*. A Special Theme Issue, **360**, 1705-1719.

Pielke R. A. Sr., Adegoke, J, O., Przekurat, A. B., Hiemstra, C., Lin, J. C., Nair, U. S., Niyogi, D. And Nobis, T. E., 2007, "An overview of regional land-use and land-cover impacts on rainfall", *Tellus B*, **59**, 3, 587-601.

Ranjan, O. J. and Anand, S., 2017, "Adaptation and Sustainability in Development: Case Study of Tawang District, Arunachal Pradesh", In (Bindhy Wasini Pandey, V. S. Negi and Poonam Kumria eds.) *Environmental Concerns and Sustainable Development in Himalaya*. Research India Press, New Delhi, 261-281.

Ranjan, O. J., Anand, S. and Pandey, B. W., 2016, "Understanding cultivation Ecology in Tawang-Chu River Basin Arunachal Pradesh", *Climate Change and Sustainable Development*. Shabdvani Prakashan, New Delhi, 189-203. https://scholar.google.com/citations?user=bsIS_YgAAAAJ&hl=en.

Ranjan, O. J., Anand, S., Pandey, B. W. and Kumria, P., 2020, "Spatial Analysis of Physio-Climatic Changes and Its Impact on Human Adaptation in Tawang Valley: A Case Study of Monpa Tribe, Eastern Himalaya", *The Eastern Anthropologist*. Serials Publication (P) Ltd. New Delhi, India, **78**, 1, 125-138. https://scholar.google.com/citations?user=bsIS_YgAAAAJ&hl=en.

Sekertekin, A., 2019, "Validation of Physical Radiative Transfer Equation-Based Land Surface Temperature Using Landsat 8 Satellite Imagery and SURFRAD *in-situ* Measurements", *Journal of Atmospheric and Solar-Terrestrial Physics*, 196, 105161. https://doi.org/10.1016/j.jastp.2019.105161.

Tahir, A. A., Chevallier, P., Arnaud, Y. and Ahmad, B., 2011, "Snow cover dynamics and hydrological regime of the Hunza River basin, Karakoram Range, Northern Pakistan", *Hydrology and Earth System Sciences*, **15**, 7, 2275-2290.

Tang, Q., Zhang, X. and Francis, J., 2014, "Extreme summer weather in northern mid-latitudes linked to a vanishing cryosphere", *Nature Climate Change*, **4**, 45-50. https://doi.org/10.1038/nclimate2065**.**

The National Aeronautics and Space Administration (n.d.). NASA POWER. NASA. Date Accessed 15.06.2021.

USGS, Landsat 8 OLI and TIRS Calibration Notices. https://www.usgs.gov/core-science-systems/nli/landsat/landsat-8-oli-and-tirs-calibration-notices.

Valovcin, F. R., 1978, "Spectral radiance of snow and clouds in the near-infrared spectral region", AFGL-TR-78-0289, ADA 063761.

Van Rooy, D. J., 1965, "Wiskunde in Suid-Afrika", *Koers - Bulletin for Christian Scholarship*, 32(7/8). https://doi.org/10.4102/koers.v32i7/8.1550.

Zhengming, Wan and Dozier, J., 1996, "A generalized split-window algorithm for retrieving land-surface temperature from space", *IEEE Transactions on Geoscience and Remote Sensing*, **34**, 4, 892-905. https://doi.org/10.1109/36.508406.